Estuarine, Coastal and Shelf Science 263 (2021) 107626

Contents lists available at ScienceDirect

Estuarine, Coastal and Shelf Science

journal homepage: www.elsevier.com/locate/ecss

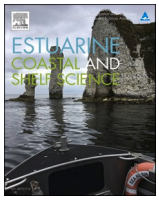

Modelling the removal of an earth bund to maximise seawater ingress into a coastal wetland

Fazlul Karim [a,*], Jim Wallace [b], Brett N. Abbott [c], Mike Nicholas [d], Nathan J. Waltham [b]

[a] CSIRO Land and Water, Black Mountain Laboratories, Canberra, ACT, 2601, Australia
[b] Centre for Tropical Water & Aquatic Ecosystem Research (TropWATER), James Cook University, Townsville, QLD, 4811, Australia
[c] CSIRO Land and Water, Australian Tropical Science and Innovation Precinct, Townsville, QLD, 4814, Australia
[d] Independent Consultant, 5 Chapman Street, Mysterton, QLD, 4812, Australia

ARTICLE INFO

Keywords:
Hydrodynamic modelling
Tide
Sea level rise
Low atmospheric pressure
Onshore wind
Wetland

ABSTRACT

Weed infestation is a critical management issue for maintaining the natural values of coastal wetlands across the world. Widespread use of herbicides to control weeds has resulted in environmental issues in the past and has led to the search for more natural control methods such as using saline water. This study investigates management options to restore the natural flow regimes between freshwater wetlands and seawater by removing a bund which was built to grow ponded pasture. The study was carried out in the Mungalla wetland in Queensland, which is an important Nywaigi aboriginal community asset for recreation, cultural and economic activities. The study used modelling and monitoring methods to (a) assess how effective the earth bund was in excluding seawater and (b) the extent to which seawater could enter the wetland without the bund. Eleven scenarios were investigated to estimate seawater ingress under different tide, onshore wind, low atmospheric pressure and sea level rise (SLR) conditions. Results show that removal of the bund reinstated periodic tidal ingress into the wetland. Seawater intrusion was also shown to increase when there were onshore winds and/or low atmospheric pressure associated with cyclones. The greatest impact was under future SLR, where large increases in the inundation frequency and extent are likely to cause a shift in the wetland vegetation towards native salt tolerant species. Findings of this study are useful for examining the potential impact of various management interventions that are being considered for wetland system repair. For example, the removal or height adjustment of tidal barriers, dredging of silted streams, removal of weeds from choked streams and reintroduction of tidal flows to control weed infestation, improve water quality and restore natural values to the wetlands.

1. Introduction

Coastal wetlands are important environmental and ecological assets as they provide significant habitats for flora and fauna often supporting commercial and recreational fisheries (Barbier, 2011; Erwin, 2009; Mitsch et al., 2015). Wetland systems may also provide important filtering services of contaminants, nutrients and sediments (McJannet et al., 2012; Mitsch et al., 2015), whilst also providing cultural and recreational benefits (Faccioli et al., 2014). Wetlands also provide important ecosystem functions, many of which have been significantly compromised by manmade activities (Gedan et al., 2009; Sheaves et al., 2012). The restriction of tidal flushing onto coastal wetlands and intersecting creeks by roads, pipelines, floodgates and culverts has negatively impacted wetland productivity and detrimentally impacted bird, fish and plant assemblages (Howe et al., 2009; Raposa and Roman, 2001). In response, there has been increasing effort in recent decades to rehabilitate coastal wetlands by removing manmade barriers (Abbott et al., 2020; Gedan et al., 2009; Teal and Weishar, 2005) and such restoration efforts will only increase following the United Nations recent declaration of a decade on ecosystem restoration (Waltham et al., 2020).

The Great Barrier Reef (GBR) lagoon of north eastern Australia has important tangible linkages with adjacent coastal wetlands and estuaries, which are connected as part of a larger nursery complex that supports many marine and freshwater aquatic species (Adams et al., 2021; GBRMPA, 2013). Many economically important fisheries have a critical estuary lifecycle phase (Sheaves et al., 2014), and rely directly on connectivity between the reef and the shallow tidal and freshwater wetland features (Sheaves et al., 2012). However, many functional

* Corresponding author.
E-mail address: Fazlul.karim@csiro.au (F. Karim).

https://doi.org/10.1016/j.ecss.2021.107626
Received 6 June 2021; Received in revised form 4 October 2021; Accepted 19 October 2021
Available online 21 October 2021

characteristics of this habitat complex are under threat due to on-going expansion of city centres for increasing population, port, industrial and agricultural expansion (Waltham and Sheaves, 2015), with runoff contributing to poor water quality and loss of natural estuarine and freshwater wetlands as nursery habitat (Arthington et al., 2020; Pearson et al., 2021; Waltham et al., 2019). Land use changes have resulted in the loss of estuarine habitats in the GBR catchments either owing to agricultural and urban expansion (Canning and Waltham, 2021), such as saltmarsh areas (Wegscheidl et al., 2017), but bunding and reclamation of tidal wetlands for ponded pasture has increased the extent of artificial freshwater habitats (Waltham et al., 2019), which provide critical habitat for many freshwater species (Canning and Waltham, 2021), though most are now heavily infested with freshwater aquatic weeds (Butler et al., 2009). Considerable effort is needed to restore and repair critical coastal wetlands (Creighton et al., 2015; Sheaves et al., 2014), and such efforts need to be supported by rigorous monitoring data and modelling works to scientifically evaluate changes in biodiversity and marine connectivity (Canning and Waltham, 2021; Wallace et al., 2020). In situations where wetland restoration efforts result in improved biodiversity or environmental outcomes, could attract major corporate or government funding – a payment for the returned ecosystem services (Canning et al., 2021). However, while removing bund walls is possible it has challenges that need careful consideration such as whether the law permits reflooding, clarification of the land and carbon rights, an understanding of the liabilities for potential impacts on adjacent land and biota, or even the costs for this clarification and approval which remain unknown in these types of projects (Bell-James and Lovelock, 2019).

Conventional methods of weed control in coastal wetlands tend to focus on mechanical dredging and chemical spraying (Veitch et al., 2007; Waltham and Fixler, 2017) with varying success, high costs and considerable negative environmental impacts (Shimeta et al., 2016). Saltwater spraying has also been shown to be effective in destroying weeds, and is more environmentally astute than chemical spraying (Veitch et al., 2007). However, few wetland restoration projects have gone as far as re-introducing seawater ingress, mainly because of uncertainties in the extent, frequency and duration of seawater ingress after removing manmade obstructions (Waltham et al., 2019). With major advancements in computational methods, hydrodynamic modelling is capable of quantifying the hydraulic flow regimes of riverine and coastal water bodies at high spatial and temporal resolution (Karim et al., 2020; Li et al., 2017; Sandbach et al., 2018). By combing this modelling technique with high resolution topography data, the duration, frequency and timing of wetland inundation can be easily quantified (Karim et al., 2020; Lopes and Dias, 2015). Hydrodynamic modelling is also an efficient way to investigate modified flow regimes due to artificial structures (Lopes and Dias, 2015; Lopes et al., 2004) and is widely used to investigate wetland inundation (Karim et al., 2012, 2014; Tuteja and Shaikh, 2009) and salinity modelling (Vale and Dias, 2011; Zahed et al., 2008), which has improved greatly the ability for managers to make more informed decisions (Mitsch et al., 2015).

This paper demonstrates how a two dimensional (2D) hydrodynamic model can be set up, calibrated and applied to investigate tidal ingress into a coastal wetland (e.g. Mungalla wetland near Ingham in north Queensland). This wetland is typical of many of the (once) tidal wetlands adjacent to the GBR lagoon that have become degraded due to the construction of an earth bund, effectively disconnecting flow with downstream estuaries. The bund led to extensive weed infestation in this wetland; largely Aleman grass (*Echinochloa polystachya*); Olive hymenachne (*Hymenachne amplexicaulis*) and para grass (*Urochloa mutica*). Weed control in the Mungalla wetland had focussed on the use of chemical spraying, which was expensive, ecologically undesirable and short lived, requiring relatively frequent respraying. It was therefore decided to investigate a more natural form of weed control method by restoring tidal ingress of seawater by removing the earth bund. However, to assess if this might work in advance of extensive earthworks, the hydrodynamic modelling simulations described here were carried out. These simulations include the time series modelling of water depth in the Mungalla wetland associated with large (king) tides with and without the earth bund in place. Simulations also include the effects of onshore winds that coincide with the king tides, as these can affect the area and extent of tidal ingress. Finally, the potential impact of SLR is also simulated to estimate how the extent, frequency and duration of tidal ingress into the wetland might change in the future.

2. Study area

This study focused on the Mungalla wetland (a complex of small and large lagoons) in north Queensland, in the downstream part of the Herbert River catchment (Fig. 1). Mungalla and its adjacent lands are drained not by the Herbert River itself but by Palm Creek which flows along the western boundary of wetlands. Palm Creek is a distributary of the Herbert River and enters the sea independently of the main channel of Herbert River, which discharges further north. Lucy Creek provides a link between the Trebonne and Palm Creeks and carries water from Trebonne to Palm Creek immediately above the Mungalla wetland. The Stone River is one of the major tributaries of the Herbert River and it also supplies freshwater to the wetland through Trebonne Creek. Mungalla wetland connects the sea through the Cassady Creek. However, tidal ingress into the wetland was obstructed because of an earthen bund (approximately 3 m high and 5 m wide) on the Cassady Creek at the downstream end of the wetland.

The Mungalla region is part of the Wet Tropics of north Queensland with average annual rainfall at Ingham of 2026 mm. The rainfall is strongly seasonal with approximately 80% of the rain falling between December and April. The months of July–October receive, on average, less than 50 mm of rain each month (Abbott et al., 2020). These rainfall characteristics determine the patterns of wetting and drying in the wetland; when they fill, when they empty, and how long they hold water. Streamflow in all tributaries and distributaries of the Herbert River are ephemeral. There is a large seasonal variation in streamflow (Fig. 2), with 93% of flow occurring in the wet-season months of December to April with the highest flow in February (36%).

Local tides are semidiurnal having one large and one small peak each day (Fig. 3). Tidal range varies from 0.1 to 4.0 m from observations between 2001 and 2016. In any year there are two 'king' tides, the highest tides, once occurs during summer (January/February), while the other occurs during winter (July/August). During the king tides there is the potential for the wetland to become inundated. Past records show that tides of 3.7 m high or more with respect to the lowest astronomical tide (LAT) have the potential to ingress into the wetland (e.g. Abbott et al., 2020).

3. Method of study

3.1. Monitoring tidal inundation

Five high frequency CTD-Diver loggers were deployed to measure water depth, barometric pressure, temperature and electrical conductivity from October 2012 to March 2017. The loggers were placed at five permanent locations in the wetland at 50, 250 and 450 m upstream, and 50 and 250 m downstream of the bund (Fig. 4). Data were captured every 15 min and used in conjunction with rainfall measured at Allingham and tide level measured at Lucinda (Fig. 1). The Mungalla wetland complex was also monitored for changes in vegetation that occurred following the removal of the earth bund in October 2012. Details of these measurements and other ecological monitoring can be found in Waltham et al. (2020) and Abbott et al. (2020).

3.2. Modelling framework

The study was conducted using a 2D flexible mesh (also called irregular grid) hydrodynamic model, commonly known as MIKE 21 FM

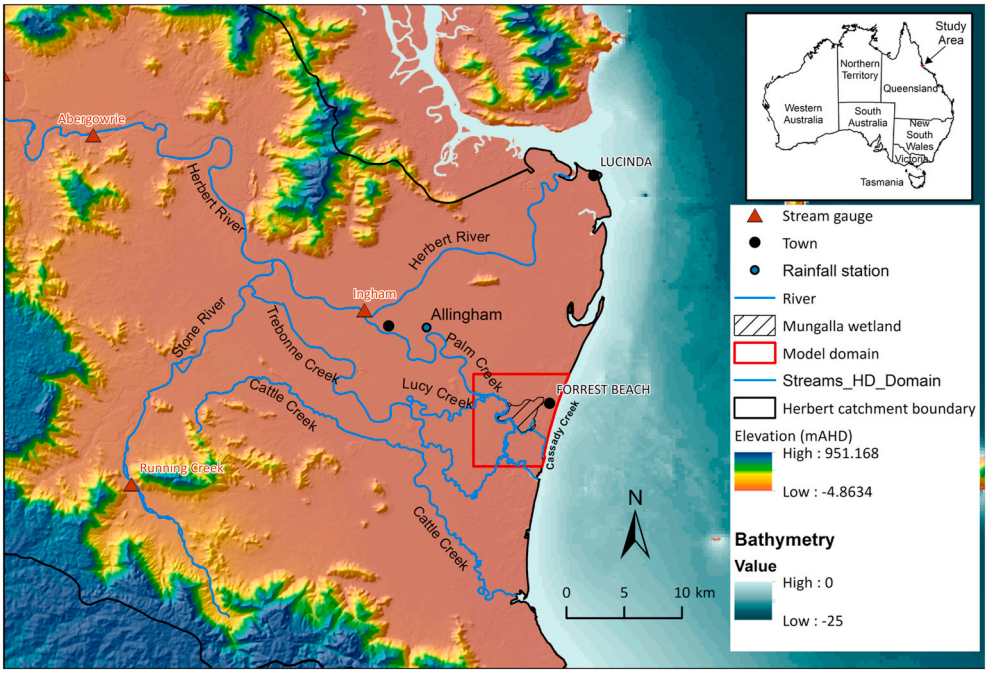

Fig. 1. Location of Mungalla wetland and stream network in the Herbert River catchment.

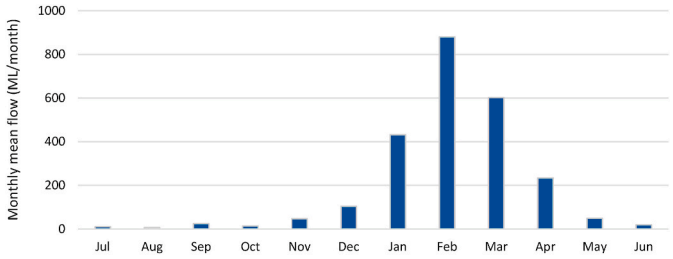

Fig. 2. Mean monthly flow at Running Creek in the Stone River based on observed flow records for the period of 1980–2018.

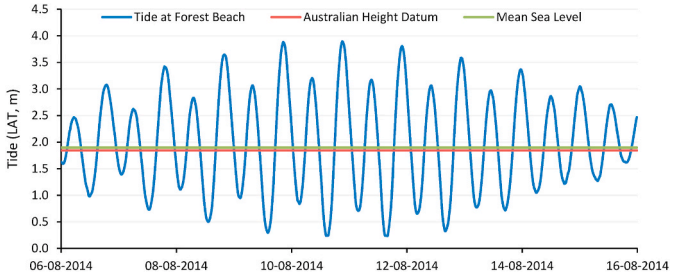

Fig. 3. An example of typical tidal cycles at Forrest Beach (3 km from the Mungalla wetland). Data are presented with respect to the LAT datum.

(DHI, 2016). The model was configured for the downstream part of the Herbert River catchment that comprises the Mungalla wetland complex and adjoining lands (Fig. 1). A physically based conceptual rainfall-runoff model (NAM) (DHI, 2008) was used to estimate inflow to the modelling domain from upstream catchments. The wetland receives freshwater through Palm and Lucy creeks during summer months (Nov–Apr). Both are ephemeral streams (May–Sept) but carry a large volume of water during floods (Jan–Mar). To assess maximum seawater ingress into the wetland, inflows from the Palm and Lucy creeks were assumed zero.

3.3. Input data

Inputs to the model were topography, surface roughness coefficients and boundary flow. Model boundaries include inflows through the Palm and Lucy Creeks and tide levels at the seaside boundary.

3.3.1. Topography

The topography data for the study area were obtained from a 30 m resolution hydrologically corrected SRTM (Shuttle Radar Topography Mission) data for the entire catchment, and a laser altimetry derived 1 m resolution LiDAR (Light Detection And Ranging) data covering the Mungalla wetland. By re-sampling the two data sets, a 10 m resolution digital elevation model (DEM) was produced for the hydrodynamic modelling domain covering an area of 66 km^2 (Fig. 1). In the re-sampling procedures, an algorithm was used to ensure stream topography as seen in the 1 m DEM was maintained in the re-sampled grids. The LiDAR DEM was further corrected using surveyed cross-sections for streams that were deemed to have contained water during the LiDAR survey. Elevations of stream grids were manually checked and adjusted at some locations, where necessary, to ensure a continuous stream until it met with another stream or open sea. A field survey was conducted to measure stream cross-sections at 18 locations between the bund and coastline along the Cassady Creek and the bathymetry of two main wetlands, Annabone and Boolgaroo (Fig. 4). These manual surveyed data were embedded into the DEM, as LiDAR doesn't penetrate to the ground surface through water or dense vegetation.

3.3.2. Roughness

Hydraulic roughness of the land surface was derived using Geoscience Australia's dynamic land cover map (Lymburner et al., 2011) and was represented in the model using Manning's roughness coefficient (n). The land use was categorised into ocean water, mangroves, saltpans, streams, riparian vegetation, wetlands, pasture, agriculture and trees. A roughness map was produced by substituting the land use code with a corresponding roughness coefficient. Initial roughness coefficients were estimated based on published literature (Chow, 1959; LWA, 2009), and a similar study for the neighbouring Tully catchment by Karim et al. (2012). These coefficients were adjusted as a part of calibration process.

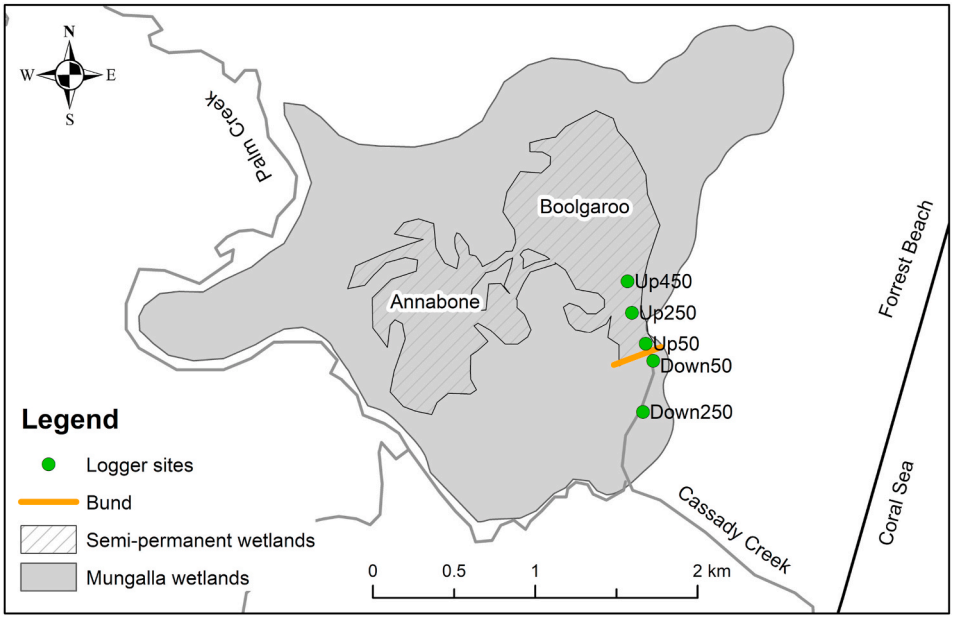

Fig. 4. Mungalla wetland complex showing location of bund and logger sites where water depths, barometric pressure, temperature and electrical conductivity were measured.

3.3.3. Boundary conditions

Two inflow boundaries were used, one receiving freshwater from the Palm Creek and the other from Lucy Creek. Both Palm and Lucy creeks are ephemeral, Palm Creek is a distributary of the Herbert River and is relatively large (~100 m wide and ~6 m deep) compared to Lucy Creek (~20 m wide and 2 m deep). A simple rainfall-runoff model was calibrated to estimate inflow through the Palm and Lucy Creeks (DHI, 2008). Initial model parameters were obtained from Karim et al. (2012) and the parameters were recalibrated for the Stone River catchment using rainfall and streamflow data recorded between 2001 and 2015 at the Running Creek (refer to Fig. 1).

Tide data were sourced from the nearest gauge at Lucinda (~20 km NE) from the Maritime Safety Queensland for the period of 2001–2015. Observed tide data for the period of September 2011 to August 2012 were used to estimate tidal constituents at Lucinda which were then used to simulate tide levels at the Mungalla coast (Forrest Beach) using the inbuilt tide analysis package in MIKE 21 (DHI, 2009). The constituents were estimated using the ISO (Institute of Ocean Science, Canada) method based on Rayleigh criterion. Once the constituents (that include 45 astronomical main constituents and 24 shallow water constituents) were estimated, high and low waters were estimated and compared with the observed tides at Lucinda. Tide levels at Mungalla were then predicted using the calibrated tidal constituents.

3.4. Model configuration and calibration

The hydrodynamic modelling domain was configured covering the Mungalla wetland and surrounding land subject to tidal inundation. Four different triangular mesh zones were used to represent the modelling domain. A very fine mesh (2–5 m^2) was used to reproduce streams in the model followed by slightly larger triangular mesh as buffers. A third category mesh of medium size was used for the floodplains that are subject to inundation. A much larger mesh size was used for the rest of the hydrodynamic model domain (Fig. 5). The final mesh consisted of 604,200 triangular mesh elements with the minimum element size of 1.86 m^2 and the maximum element size of 6200 m^2. A smooth transition between two mesh zones was maintained by enforcing a minimum angle of 30° for every mesh element. The upstream boundary of the hydrodynamic model was set well above the tidal inundation to avoid any impact of boundary conditions.

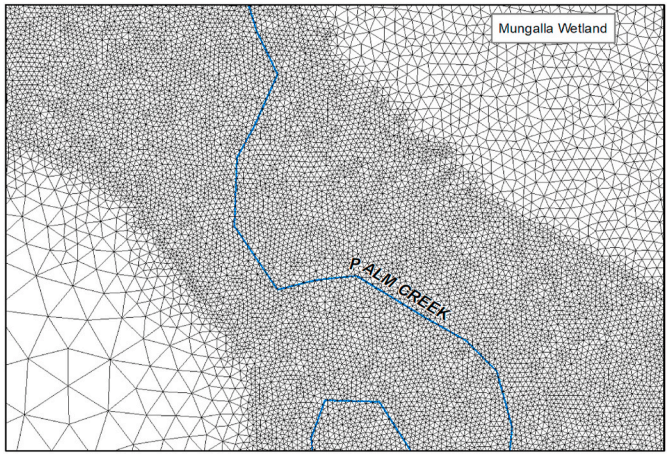

Fig. 5. An example of flexible mesh hydrodynamic modelling configuration with variable mesh size.

For calibration and scenario modelling, a computational time increment was derived after satisfying numerical stability criteria. A time step of 1 s was used as this produced a stable solution for the largest recorded tide (4.1 m) and large inflow conditions. Simulation of each model was carried out for 4–5 days covering all tides greater or equal to 3 m that have potential to reach the logger at 450 m downstream of the bund. The models were run using GPU (graphics processing unit) machines consisting of 16 CPU cores and 3 GPU cards. For each run, it took about 6 h of computer time to simulate 5 days of a tidal event. At the seaside boundary, 15 min interval observed tide levels were specified. The model uses an inbuilt interpolation technique to derive tide level at each computational time step. At the two inflow boundaries, daily time series of discharge were specified. While the model has the option of producing output at any time interval, simulated water depths in this study were recorded at an hourly interval and at some selected locations, half-hourly. These data were then used to estimate the tidal influences in and around the wetland.

Model calibration is an important part of hydrodynamic modelling as it provides not only the realistic representation of the physical systems

but also the reliability and confidence in the predicted results. At first, the model was calibrated for the tidal constituents and then for simulations of tidal ingress into the wetland. The MIKE 21 FM model parameters were calibrated against a large tide (4.1 m) occurring in January 2014. Observed tide data from the five automatic loggers that gave continuous water elevations were used to constrain the model parameters. The main calibration parameter was the roughness coefficient, Manning's n, and the eddy viscosity. Model performance in simulating tidal intrusion to wetlands was evaluated using a comparison of tide levels at 250 and 450 m upstream of the bund.

3.5. Scenario modelling

A total of eleven scenarios were modelled to estimate inundation extent across the wetland under tidal influence for the present and future conditions. These include one scenario for bund, four for wave heights, two for onshore winds, two for low atmospheric pressure and two for SLR (Table 1). Onshore wind produces waves that increase the effective tide height at the coast and the extent of tidal flow over the land. Using the relationship between wind speed and wave height, we have simulated the impact of 5 and 10 m/s onshore winds. The north Queensland coast is also subject to cyclones during the summer and if these coincide with high tides, low pressure associated with cyclone can cause an increase in sea level. Studies of the effect of atmospheric pressure and sea level indicate that sea level increases by ~1 cm per mb pressure below the standard atmospheric pressure of 1013 mb (Gaspar and Ponte, 1997). During a cyclone the atmospheric pressure can drop to ~950 mb, causing a SLR of approximately 0.6 m. Finally, it is predicted that sea level along the Queensland coast may rise by 0.5 m by 2060 and as much as 0.8 m by 2100 (Zhang et al., 2017). For each of the above scenarios the extent of inundation and volume of seawater ingress into the wetland (with no bund in place) was estimated.

4. Results

4.1. Tidal ingress into the wetland

An example of simulated tidal ingress into the wetland along with observed tide level for a calibration run is shown in Fig. 6 for a 4.1 m high tide. In general, model simulations match well with observed tide levels both upstream and downstream of the bund. The magnitude and timing of peak depths is well reproduced, although the rate at which simulated depth declines after the peaks is more rapid than observed, especially for the two loggers upstream of the bund. The latter difference should have little effect on the simulation of the timing and maximum volume of seawater ingress within the wetland.

Simulated water depths in the wetland were verified against two other tides of 3.9 and 4.0 m (Fig. 7). In these runs, the model parameters were left as in the calibration run and no further adjustments were made. Again, the model reproduced the magnitude and timing of peaks well. This gives confidence in the ability of the model to predict the timing and size of peak seawater depth and its maximum volume for a range of future tide heights.

The frequency of tidal ingress into the wetland was estimated using the observed water depth and electrical conductivity data collected from 5 logger sites across the wetland (refer to Fig. 4). Results showed that tides of 3.7 m high or greater (at nearby Forrest Beach) have the potential to intrude into the wetland. To assess the frequency of tidal inundation of the wetland a list of all high tides >3.7 m from January 2012 to March 2017 were investigated (Fig. 8).

Results show that there are about 18 days per year when tide height is greater than 3.7 m that has the potential to reach upstream of bund location. These tend to occur for a period of 2–3 consecutive days, so the wetland inundation frequency per event is between 6 and 10 times a year. Inundation frequency is less for larger tides (Table 2). For example, only 0 to 5 tides of greater than 4.1 m occurred each year (average ~ 2 per year), which would usually occur in a single annual event.

Table 1
List of tidal scenarios that were investigated for wetland inundation.

Scenario	Bund wall	Tide height	Wind speed	Atmospheric pressure	Wave height increase	SLR
		(m)	(m/s)	(mb)	(m)	(m)
1	Present	4.3	0	1013	0	0
2	Absent	4.3	0	1013	0	0
3	Absent	4.1	0	1013	0	0
4	Absent	3.9	0	1013	0	0
5	Absent	3.7	0	1013	0	0
6	Absent	4.3	5	1013	0.7	0
7	Absent	4.3	10	1013	2.1	0
8	Absent	4.3	0	950	0	0.6
9	Absent	3.7	0	950	0	0.6
10	Absent	3.9	0	1013	0	0.5
11	Absent	3.9	0	1013	0	0.8

4.2. Effect of bund removal

The bund in the downstream end of the Mungalla wetland was found to be a barrier for the seawater ingress into the wetland. While a 3.7 m tide reaches the bund, simulations show that the bund prevented seawater ingress to the wetland for even the largest recorded tide of 4.3 m (Fig. 9a). The comparative simulation for the same tide without the bund in place shows extensive seawater ingress and a large area of inundation, ~55 ha (Fig. 9b and Table 3). Without the bund, seawater is estimated to reach approximately 180 m above the bund for a 3.9 m tide, 780 m for a 4.1 m tide, and 1150 m for a 4.3 m tide respectively– though all were unable to reach the Annabone regions (see Fig. 4 for location). At these high tides, the freshwater hydraulic barrier was negligible.

The simulation for the 3.7 m tide is not shown as it produced very little inundation within the wetland (Table 3) and no seawater entered beyond the bund. A 3.9 m tide caused tidal ingress above the bund with a small area of inundation (4.4 ha; Table 3). More significant tidal ingress into the wetland occurred with 4.1 m tide, however, the extent of inundation is confined along a narrow stretch of the wetland. While the 4.3 m tide inundates a large part of Boolgaroo lagoon (55 ha), it doesn't reach to the Annabone area in the western part of the wetland (Fig. 9b). Seawater entered 180 m beyond the bund location for the 3.9 m tide and even further for larger tides, with maximum distance of 1150 m under the highest 4.3 m tide. Freshwater quantity and flow into the wetland during these simulations was almost negligible.

The total amount of seawater entering the wetland ranged from 125 m^3 (for the 3.7 m tide) to 118,060 m^3 (for the 4.3 m tide). The concurrent amounts of salt in the seawater (calculated using the average salt concentration of 35 g/L), would be 4.4–4132 tonnes.

4.3. Effects of onshore wind

Moderate onshore breezes (5 m/s) were estimated to produce a wave height of 0.7 m. When added to the high tide simulations of 3.7 and 4.3 m, the increased inundation was small with an average increase of 0.1 and 1.5 ha respectively (Fig. 10a). However, strong onshore winds (10 m/s) produced waves approximately 2.1 m high, which when coincided with high tide simulations of 3.7 and 4.3 m, is predicted to cause large increases in seawater inundation in the wetland (Table 4). For example, a 10 m/s onshore wind with a 4.3 m high tide was predicted to increase inundation extent by 200%, with seawater reaching well into the Annabone area (Fig. 10b).

4.4. Effects of low pressure system

Low atmospheric pressure of 950 hPa is predicted to increase sea

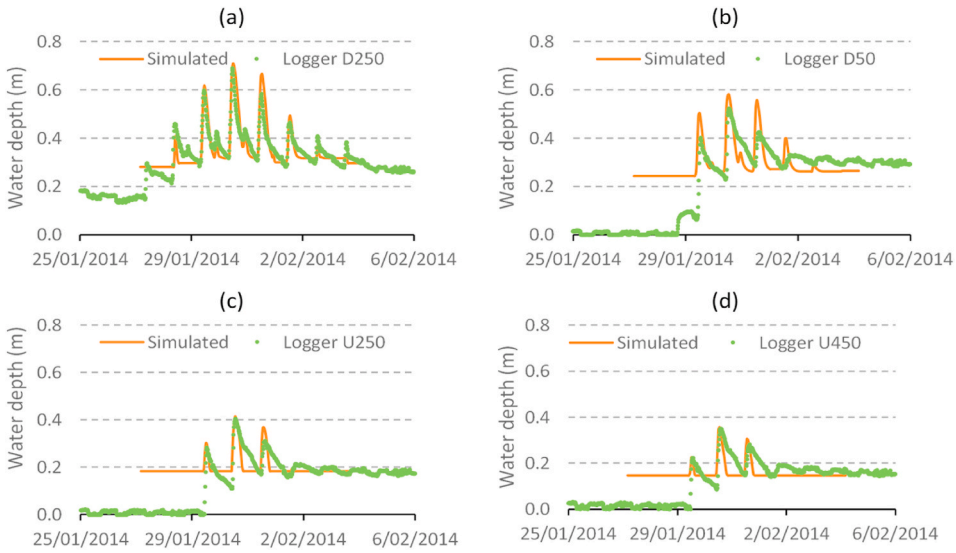

Fig. 6. Observed (green dots) and simulated (orange line) water depths for a 4.1 m tide at (a) 250 m and (b) 50 m downstream of the bund, and (c) 250 m and (d) 450 m upstream the bund. (For interpretation of the references to colour in this figure legend, the reader is referred to the Web version of this article.)

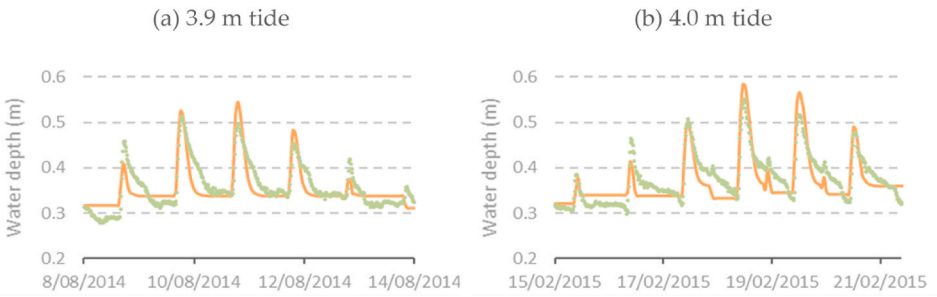

Fig. 7. Comparison between observed (green dots) and simulated (orange line) water depths at 250 m below the bund for the tides of (a) 3.9 m in August 2014 and (b) 4.0 m in February 2015. (For interpretation of the references to colour in this figure legend, the reader is referred to the Web version of this article.)

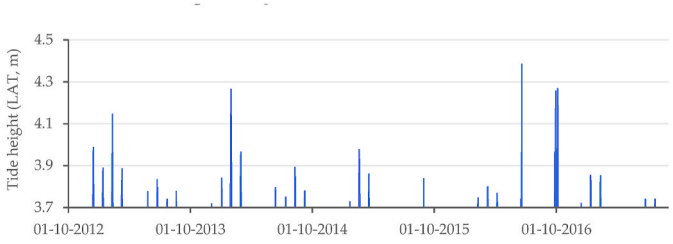

Fig. 8. Observed tide at Forrest Beach since 2012 that are greater than 3.7 m. Data are presented with respect to LAT datum which is 1.844 m below Australian Height Datum (AHD) and 1.897 m below Mean Sea Level (MSL).

Table 2
Number of tides per year greater than 3.7–4.1 m at Forrest Beach (3 km from the Mungalla wetland).

Year	Tide >3.7 m	Tide >3.9 m	Tide >4.0 m	Tide >4.1 m
2012	11	6	2	0
2013	22	8	3	1
2014	19	11	6	3
2016	23	10	9	5

level by approximately 0.6 m. If this occurs along with high tides then there is a marked increases inundation area (Table 5). For example, low pressure increases inundation area when there is a 3.7 m tide from 0.17 to 55 ha. For a 4.3m, the increase is from 55 to 353 ha, with the seawater spreading 2370 m into the wetland and flooding almost the entire wetlands (Fig. 11).

With low atmospheric pressure, the total amount of seawater entering the wetland ranged from 118,395 m^3 (for the 3.7 m tide) to 1,928,215 m^3 (for the 4.3 m tide). The concurrent amounts of salt in the seawater (calculated using the average salt concentration of 35 g/L), would be 4144 to 67,488 tonnes.

4.5. *Effects of sea level rise*

The addition of SLR to high tides substantially increased the extent of inundation. A SLR of 0.5 m meant that a 3.7 m tide, which normally would not enter the wetland, would now reach over 1 km into the wetland and inundate ~54 ha (Table 6). A higher SLR of 0.8 m with this tide would inundate 254 ha, with depths increasing from 0.5 m to 1 m. The highest inundation occurs with a 4.3 m tide and SLR of 0.8 m resulting in flooding of the entire wetland (423 ha) to depths of up to 1.5 m.

Very large amounts of seawater and salt enter the wetland under the above scenarios, ranging from 113,000 m^3 with ~4000 tonnes of salt to a massive 3.4 million m^3 with ~120,000 tonnes of salt. Note that most, but not all, of this salt leaves the wetland as the high tides recede.

Clearly SLR has a major effect on the ingress of saltwater into the wetland, however, another important effect occurs by the frequency with which this occurs. Daily maximum tide data show that tides over 2 m occur every day, with higher tides occurring less often and none are

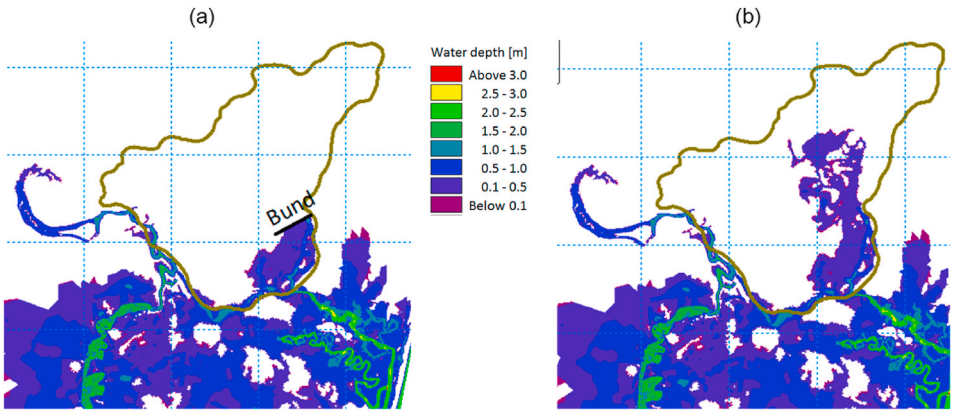

Fig. 9. Impact of the bund on wetland inundation for a 4.3 m tide, (a) inundation with an earth bund, (b) inundation without the bund.

Table 3
Effect of tide height on seawater ingress and inundation depth in the wetland. Presented are the distance of tidal ingress (m), area inundated (ha), the total volume of seawater ingress (m^3), and the mass of salt introduced to the wetland (tonnes).

Tide height (m)	Distance above bund (m)	Total Area inundated (ha)	Volume of seawater ingress (m^3)	Influx salt mass in wetland (tonnes)
3.7	15	0.17	125	4.4
3.9	180	4.36	4810	168
4.1	780	16.81	26755	936
4.3	1150	55.02	118060	4132

above 4.4 m (Fig. 12). A 3.7 m tide is sufficient to reach the location of the earth bund under current sea level conditions and this occurs on ~18 days per year (5% of the time). If sea level rose by 0.5 m, then a 3.2 m tide would reach the bund, and this would occur 128 days per year (35% of the time) (Fig. 12). For higher SLR of 0.8 m, a 2.9 m tide would reach the bund, and this would occur 231 days per year (63% of the time).

5. Discussion

The hydrodynamic model (MIKE 21 FM) used to simulate seawater inundation in the Mungalla wetlands was found to be a reliable modelling tool to investigate tidal dynamics in this type of coastal wetland. The study confirms that removal of the earth bund restored periodic tidal ingress into the wetland. Seawater intrusion was also shown to increase when there were onshore winds and/or low atmospheric pressure associated with cyclones. The greatest impact on seawater flooding was under future SLR, where large increases in the flood frequency and extent are likely to cause a shift in the wetland inundation. The accuracy of predicted tide levels in the wetland is in the range of a few centimetres. However, this high level of confidence relies on careful calibration of model parameters using observed tide levels at multiple locations. Accurate modelling is also dependent on the availability of high-resolution topography data (i.e. 1 m LiDAR DEM) as this was found to be the most sensitive input (Cook and Merwade, 2009; Lamichhane and Sharma, 2018). Detail topographic data also allow us to more accurately represent artificial barriers and small rivers and creeks connecting the coastal wetlands with the sea using a flexible mesh model. This had the advantage of reducing the computation time in addition to improving the accuracy of model predictions (Bomers et al., 2019; Hoch et al., 2018).

The presence of the earth bund prevented seawater entering the Mungalla wetland beyond the earth wall, even for the highest tides of 4.3 m. When it was removed tides higher than 3.7 m were then able to enter the wetland, inundating progressively larger areas as the tide height increased to 4.3 m, when ~12.5% of the wetland was flooded to a depth of ~0.5 m. Although this tide inundated a large part of Boolgaroo lagoon, it didn't reach the Annabone area in the western part of the wetland. Large volumes of seawater (up to 118060 m^3) containing large amounts of salt (up to 4132 tonnes) entered the wetland, but much of this would have drained from the wetland as the high tides receded.

When onshore winds coincide with high tides there can be substantial increases in wetland inundation. Whereas moderate breezes (up to 5 m/s) cause little increase in inundation area, strong winds (~10 m/s) increase the area inundated by 200% and the volume of water entering the wetland by over 400%. Under these conditions the highly weed infested Annabone part of the wetland would also be inundated with

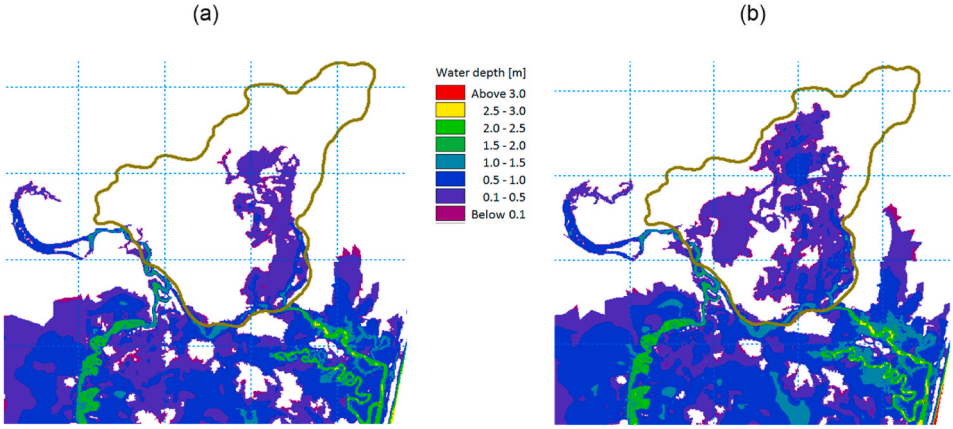

Fig. 10. Wetland inundation scenarios for different tides and onshore winds, (a) 4.3 m tide and 5 m/s wind speed, (b) 4.3 m tide and 10 m/s wind speed.

Table 4
Effect of onshore wind on seawater ingress and inundation depth in the Mungalla wetland. Presented are the distance of tidal ingress (m), area inundated (ha), the total volume of seawater ingress (m^3), and the mass of salt introduced to the wetland (tonnes).

Variable	3.7 m tide			4.3 m tide		
	No wind	Wind 5 m/s	Wind 10 m/s	No wind	Wind 5 m/s	Wind 10 m/s
Distance above bund (m)	15	25	120	1150	1190	1750
Total Area inundated (ha)	0.17	0.25	2.63	55.02	56.51	165.34
Volume of seawater ingress (m^3)	125	195	2875	118,060	123,805	488,870
Salt mass in wetland (tonnes)	4.4	6.8	101	4132	4333	17,110

Table 5
Effect of low atmospheric pressure on seawater ingress and inundation depth (AtmP: atmospheric pressure).

Variable	3.7 m tide		4.3 m tide	
	AtmP 1013 mb	AtmP 950 mb	AtmP 1013 mb	AtmP 950 mb
Distance above bund (m)	15	1155	1150	2370
Total Area inundated (ha)	0.17	55.29	55.02	353.31
Volume of seawater ingress (m^3)	125	118,395	118,060	1,928,215
Salt mass in wetland (tonnes)	4.4	4144	4132	67,488

seawater.

The coincidence of high tides with low atmospheric pressure (950 hPa) associated with cyclonic conditions leads to larger extent of seawater movement into the wetland. A low pressure, with a 3.7 m tide, causes inundation similar to that under a 4.3 m tide with normal atmospheric pressure. A more serious scenario is when low pressure coincides with the higher 4.3 m tide, when 353 ha (~80%) of the wetland is inundated to a depth of up to 1.1 m with seawater travelling 2370 m upstream from the bund location.

Simulation of SLR shows that seawater enters the wetland (above the bund) with tides that previously did not reach it. For example, where a 3.7 m tide does not currently enter the wetland it will cause significant flooding with a 0.5 m SLR which is expected to occur by 2060 and beyond. This also implies that tides lower than this, will also reach the wetland and will occur much more frequently in the future. For example, a 3.2 m tide occurs 128 days per year compared to only 18 days per year for a 3.7 m tide. Should SLR by 0.8 m by 2100, seawater ingress into the wetland increases even further. In this scenario a 2.9 m tide would reach the wetland and would occur 231 days per year. The frequency of rare high tides of 4.3 m, which currently occur ~ once every 5 years, would increase to 49 days per year causing massive ingress of seawater and deep flooding of the entire wetland. While these results are specific to the Mungalla wetland, the modelling approach and modelling framework can be applied to many other disconnected coastal wetlands, thereby providing a very useful tool for the a priori evaluation of the effect of removing (or introducing) manmade barriers to tidal movement as well as the impacts of future SLR on coastal inundation.

The removal of the earth bund in the Mungalla wetland was predicted to allow much more frequent ingress of seawater. This was indeed found to be the case shortly after when the bund was removed in October 2012 (Abbott et al., 2020). A high tide of 4.3 m inundated much of the wetland in January 2013 and this had the desired effect of greatly reducing freshwater invasive weeds such as Para grass (*Urochloa mutica*), Aleman grass (*Echinochloa polystachya*) and Hymenachne (*Hymenachne amplexicaulis*) This in turn allowed native salt tolerant vegetation to regrow (Abbott et al., 2020). Seawater ingress continued in subsequent years contributing improvements in water quality, most notably dissolved oxygen and pH which, in turn, led to improved fish habitats, including the presence of the Barramundi (*Lates calcifer*), an economically important species in Australia (Waltham et al., 2020). However, water quality and weed composition oscillates depending on summer rainfall. When this is high, deep freshwater in the wetland prevents the ingress of seawater and freshwater weeds can return, while when rainfall is low, seawater intrudes more frequently, and native salt

Table 6
Effect of SLR on seawater ingress and wetland inundation depth. Presented are the distance of tidal ingress (m), area inundated (ha), the total volume of seawater ingress (m^3), and the mass of salt introduced to the wetland (tonnes).

Variable	3.7 m tide		4.3 m tide	
	50 cm SLR	80 cm SLR	50 cm SLR	80 cm SLR
Distance above bund (m)	1010	1750	2340	2560
Maximum depth (m)	0.5	0.9	1.1	1.5
Total Area inundated (ha)	53.8	254.3	346.3	422.5
Volume of seawater ingress (m^3)	113,060	994,350	1,852,000	3,414,365
Weight of salt in wetland (tonnes)	3957	34,802	64,820	119,503

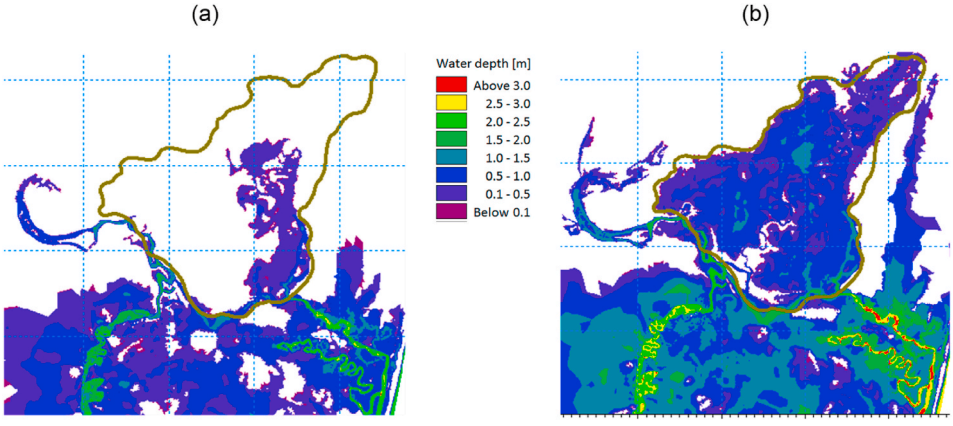

Fig. 11. Wetland inundation for a low pressure system (950 hPa): (a) 0.6 surge coincides with a 3.7 m tide, (b) 0.6 surge coincides with a 4.3 m tide.

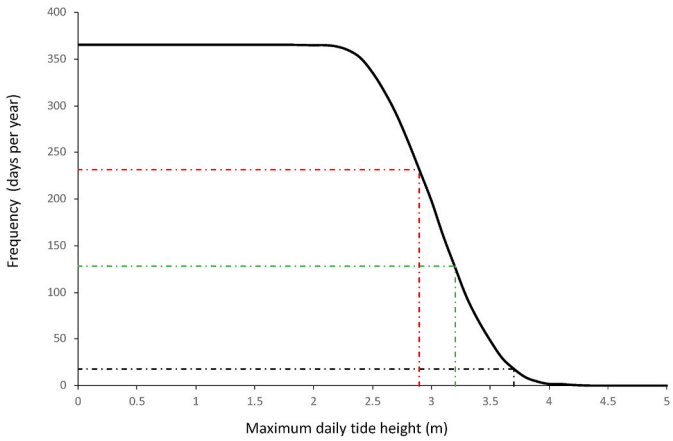

Fig. 12. Variation in the frequency of daily maximum tides with tide height. Also shown are the number of days per year for a 3.7 m tide (a) without SLR (black), (b) with SLR of 0.5 m (green), (c) with SLR of 0.8 m (red). (For interpretation of the references to colour in this figure legend, the reader is referred to the Web version of this article.)

tolerant vegetation takes over. However, it is clear that the removal of the earth bund provided a natural and more sustainable means of controlling the freshwater weeds that had infested this wetland. Bund removal also led to reconnection of the wetland to the estuary and ocean, thereby enhancing fish passage and increasing water quality.

SLR will have a major effect on the wetland as there will be a very large increase in the frequency and depth of seawater flooding. Deep seawater floods have been shown to greatly reduce the occurrence of undesirable freshwater weeds (Abbott et al., 2020) and if these floods occur multiple times per year in the future this should ultimately lead to a large and perhaps permanent shift towards native salt tolerant vegetation.

An important consideration with the modelling results here relates to the potential for bund wall removal to reconnect the coastal seascape for the purposes of enabling blue carbon opportunities (Adams et al., 2021; Duarte de Paula Costa et al., 2021). In Australia, the Clean Energy Regulator is currently developing a Blue Carbon method to activate new market mechanisms to open payment pathways from industry and investment schemes to fund restoration of coastal wetlands, including mangroves and saltmarsh (Clean Energy Regulator, 2021). To be successful, blue carbon projects need to overcome a number of barriers (Stewart-Sinclair et al., 2020) including access to local data and ecosystem services held by wetlands. In general, ecosystem services take time to re-establish, including responding to SLR, and mature which means it could take years for carbon sequestration reaches rates similar to natural wetland (Lovelock and Reef, 2020; Rogers et al., 2019). The modelling here provides an example that under future sea level the number and duration of saltwater ingress will be much higher than the present time, which could mean this restoration site becomes a blue carbon restoration project site in the future. However, the success here might indeed be cognisant on catchment hydrology where wet years might limit ingress (Abbott et al., 2020).

Another service that this wetland presents in the future, with increasing seawater ingress and connection, is greater access to the wetland by local estuarine fish species (Shervette et al., 2007). Several local estuarine fish species have a life cycle that requires floodplain connection during critical growth stages (Sheaves, 2009; Sheaves and Johnston, 2009). An example is the barramundi (*Lates calcarifer*) which has only recently been recorded in the wetland shortly after bund wall removal (Abbott et al., 2020). The presence of this fish species in the wetland, upstream of the bund wall, presents a case for restoration success, though this access is influenced by the frequency and duration of connection, which might increase in the future under climate change and SLR. On-going surveillance monitoring of fish in the restored wetland will provide details to examine this prediction.

6. Conclusions

We have clearly demonstrated the utility of hydrodynamic modelling for examining the potential impact of various management interventions that are being considered for wetland system repair. These include the removal or height adjustment for tidal barriers, dredging of silted streams along the coast and/or the removal of weeds from choked streams. In the Mungalla wetland the removal of the earth bund has reintroduced tidal flows resulting in improvement in water quality, which has helped controlling freshwater weeds. This is an environmentally acceptable approach to weed control than previous chemical spray method. The method is also sustainable in the longer term and requires little or no ongoing maintenance.

Simulations of the effect of future SLR indicate that the wetland vegetation will shift to native salt tolerant species as the frequency and extent of seawater flooding increases. This will have significant environmental and ecological benefits in terms of water quality improvement and fish biodiversity. Although the model set up and simulations in this paper are specific to the Mungalla wetland the method can be applied to many other coastal wetlands, thereby providing a very useful modelling framework for the a priori evaluation of the effect of removing (or introducing) manmade barriers to tidal movement.

Author statement

Fazlul Karim: developed the study framework and led writing of the manuscript, executed hydrodynamic modelling (HD) works and prepared figures. Jim Wallace: conceptualized and developed the methodology, supervised HD modelling works and field experiments, significantly contributed to manuscript writing. Brett Abbott: conceptualized field experiment, installed data logger, collected and processed logger data, contributed to manuscript writing. Mike Nicholas: conceptualized field experiment, installed data logger, executed field survey and contributed to manuscript writing. Nathan Waltham: conceptualized and developed the methodology, interpreted the logger data, contributed to manuscript writing.

Declaration of competing interest

The authors declare that they have no known competing financial interests or personal relationships that could have appeared to influence the work reported in this paper.

Acknowledgments

This study was carried out on the traditional lands of the Nywaigi Aboriginal people and we wish to acknowledge them as Traditional Owners, and pay our respect to their elders, past, present, and future emerging. We are thankful to Mr. Jacob Cassady, Manager of the Mungalla Station, for his support and encouragement throughout the project. This research was funded by the Australian Government Department of Agriculture, Water and the Environment under the National Environmental Science Program. We acknowledge the supply of tide data by the Maritime Safety Queensland and stream flow data by the Department of Environment and Science of Queensland Government.

References

Abbott, B.N., Wallace, J., Nicholas, D.M., Karim, F., Waltham, N.J., 2020. Bund removal to re-establish tidal flow, remove aquatic weeds and restore coastal wetland services-North Queensland, Australia. PLoS One 15.

Adams, J.B., de Freitas, D.M., Rogers, K., Woodroffe, C.D., 2021. Estuaries and coastal wetlands of the southern hemisphere – an overview. Estuarine. Coast. Shelf Sci. 250.

Arthington, A.H., Pearson, R.G., Godfrey, P.C., Karim, F., Wallace, J., 2020. Integrating freshwater wetland science into planning for Great Barrier Reef sustainability. Aquat. Conserv. 30, 1727–1733.
Barbier, E.B., 2011. Wetlands as natural assets. Hydrol. Sci. J. 56, 1360–1373.
Bell-James, J., Lovelock, C.E., 2019. Legal barriers and enablers for reintroducing tides: an Australian case study in reconverting ponded pasture for climate change mitigation. Land Use Pol. 88, 104192.
Bomers, A., Schielen, R.M.J., Hulscher, S.J.M.H., 2019. The influence of grid shape and grid size on hydraulic river modelling performance. Environ. Fluid Mech. 19, 1273–1294.
Butler, B., Dominica, L., Damien, B., Glenn, M., 2009. In: Research, A.C.f.T.F. (Ed.), Aquatic Ecology Assessment of Mungalla Wetlands. James Cook University, Townsville, p. 92.
Canning, A., Waltham, N.J., 2021. The influence of survey bias in assessing the ecological impacts of climate change and habitat loss on vertebrate assemblages across the Great Barrier Reef catchment wetlands. Ecol. Evol. 11, 5244–5254.
Canning, A.D., Jarvis, D., Costanza, R., Hasan, S., Smart, J.C., Finisdore, J., Lovelock, C. E., Greenhalgh, S., Marr, H.M., Beck, M.W., Gillies, C.L., 2021. Financial incentives for large-scale wetland restoration: beyond markets to common asset trusts. One Earth 4, 937–950.
Chow, V.T., 1959. Open Channel Hydraulics. McGraw-Hill International Edition, Singapore.
Clean Energy Regulator, 2021. Emissions Reduction Fund: Method Development. Clean Energy Regulator. http://www.cleanenergyregulator.gov.au/ERF/Pages/Method-development.aspx. (Accessed 5 May 2021).
Cook, A., Merwade, V., 2009. Effect of topographic data, geometric configuration and modeling approach on flood inundation mapping. J. Hydrol 377, 131–142.
Creighton, C., Boon, P.I., Brookes, J.D., Sheaves, M., 2015. Repairing Australia's estuaries for improved fisheries production – what benefits, at what cost? Mar. Freshw. Res. 66, 493.
DHI, 2008. NAM Technical Reference and Model Documentation. DHI Water and Environment Pty Ltd, Horsholm, Denmark, p. 96.
DHI, 2009. Tide Analysis and Prediction Module, Scientific Documentation. DHI Water and Environment Pty Ltd, Horsholm, Denmark, p. 64.
DHI, 2016. MIKE21 Flow Model FM, Hydrodynamic Module, User Guide. DHI Water and Environment Pty Ltd, Horsholm, Denmark, p. 148.
Duarte de Paula Costa, M., Lovelock, C.E., Waltham, N.J., Young, M., Adame, M.F., Bryant, C.V., Butler, D., Green, D., Rasheed, M.A., Salinas, C., Serrano, O., York, P. H., Whitt, A.A., Macreadie, P.I., 2021. Current and future carbon stocks in coastal wetlands within the Great Barrier Reef catchments. Global Change Biol. 27, 3257–3271.
Erwin, K.L., 2009. Wetlands and global climate change: the role of wetland restoration in a changing world. Wetl. Ecol. Manag. 17, 71–84.
Faccioli, M., Riera Font, A., Torres Figuerola, C.M., 2014. Valuing the recreational benefits of wetland adaptation to climate change: a trade-off between species' abundance and diversity. Environ. Manag. 55, 550–563.
Gaspar, P., Ponte, R.M., 1997. Relation between sea level and barometric pressure determined from altimeter data and model simulations. J. Geophys. Res. Oceans 102, 961–971.
GBRMPA, 2013. Coastal Ecosystems Management - Case Study: Water Quality Management. GBRMPA. Australian Government, Townsville.
Gedan, K.B., Silliman, B., Bertness, M., 2009. Centuries of human-driven change in salt marsh ecosystems. Annu Rev Mar Sci 1, 117–141.
Hoch, J.M., van Beek, R., Winsemius, H.C., Bierkens, M.F.P., 2018. Benchmarking flexible meshes and regular grids for large-scale fluvial inundation modelling. Adv. Water Resour. 121, 350–360.
Howe, A.J., Rodríguez, J.F., Saco, P.M., 2009. Surface evolution and carbon sequestration in disturbed and undisturbed wetland soils of the Hunter estuary, southeast Australia. Estuar. Coast Shelf Sci. 84, 75–83.
Karim, F., Kinsey-Henderson, A., Wallace, J., Arthington, A.H., Pearson, R.G., 2012. Modelling wetland connectivity during overbank flooding in a tropical floodplain in north Queensland, Australia. Hydrol. Process. 26, 2710–2723.
Karim, F., Kinsey-Henderson, A., Wallace, J., Godfrey, P., Arthington, A.H., Pearson, R. G., 2014. Modelling hydrological connectivity of tropical floodplain wetlands via a combined natural and artificial stream network. Hydrol. Process. 28, 5696–5710.
Karim, F., Marvanek, S., Merrin, L.E., Nielsen, D., Hughes, J., Stratford, D., Pollino, C., 2020. Modelling flood-induced wetland connectivity and impacts of climate change and dam. Water 12.
Lamichhane, N., Sharma, S., 2018. Effect of input data in hydraulic modeling for flood warning systems. Hydrol. Sci. J. 63, 938–956.
Li, J., Zhu, L., Zhang, S., 2017. Numerical model on the flow dynamics around the sediment-water interface in the tidal coastal area. Estuar. Coast Shelf Sci. 194, 57–65.
Lopes, C.L., Dias, J.M., 2015. Tidal dynamics in a changing lagoon: flooding or not flooding the marginal regions. Estuar. Coast Shelf Sci. 167, 14–24.
Lopes, L.F.G., Carmo, J.A.D., Cortes, R.M.V., Oliveira, D., 2004. Hydrodynamics and water quality modelling in a regulated river segment: application on the instream flow definition. Ecol. Model. 173, 197–218.
Lovelock, C.E., Reef, R., 2020. Variable impacts of climate change on blue carbon. One Earth 3, 195–211.
LWA, 2009. An Australian Handbook of Stream Roughness Coefficients Land and Water Australia, p. 28. Canberra.
Lymburner, L., Tan, P., Mueller, N., Thackway, R., Lewis, A., Thankappan, M., Randall, L., Islam, A., Senarath, U., 2011. The National Dynamic Land Cover Dataset. Geoscience Australia, Canberra, p. 105.
McJannet, D., Wallace, J., Keen, R., Hawdon, A., Kemei, J., 2012. The filtering capacity of a tropical riverine wetland: II. Sediment and nutrient balances. Hydrol. Process. 26, 53–72.
Mitsch, W.J., Bernal, B., Hernandez, M.E., 2015. Ecosystem services of wetlands. International journal of biodiversity science. Ecosys. Services Manag. 11, 1–4.
Pearson, R.G., Connolly, N.M., Davis, A.M., Brodie, J.E., 2021. Fresh waters and estuaries of the Great Barrier Reef catchment: effects and management of anthropogenic disturbance on biodiversity, ecology and connectivity. Mar. Pollut. Bull. 166, 112194.
Raposa, K.B., Roman, C.T., 2001. Seasonal habitat-use patterns of nekton in a tide-restricted and unrestricted New England salt marsh. Wetlands 21, 451–461.
Rogers, K., Kelleway, J.J., Saintilan, N., Megonigal, J.P., Adams, J.B., Holmquist, J.R., Lu, M., Schile-Beers, L., Zawadzki, A., Mazumder, D., Woodroffe, C.D., 2019. Wetland carbon storage controlled by millennial-scale variation in relative sea-level rise. Nature 567, 91.
Sandbach, S.D., Nicholas, A.P., Ashworth, P.J., Best, J.L., Keevil, C.E., Parsons, D.R., Prokocki, E.W., Simpson, C.J., 2018. Hydrodynamic modelling of tidal-fluvial flows in a large river estuary. Estuar. Coast Shelf Sci. 212, 176–188.
Sheaves, M., 2009. Consequences of ecological connectivity: the coastal ecosystem mosaic. Mar. Ecol. Prog. Ser. 391, 107–115.
Sheaves, M., Johnston, R., 2009. Ecological drivers of spatial variability among fish fauna of 21 tropical Australian estuaries. Mar. Ecol. Prog. Ser. 385, 245–260.
Sheaves, M., Johnston, R., Connolly, R.M., 2012. Fish assemblages as indicators of estuary ecosystem health. Wetl. Ecol. Manag. 20, 477–490.
Sheaves, M., Brookes, J., Coles, R., Freckelton, M., Groves, P., Johnston, R., Winberg, P., 2014. Repair and revitalisation of Australia's tropical estuaries and coastal wetlands: opportunities and constraints for the reinstatement of lost function and productivity. Mar. Pol. 47, 23–38.
Shervette, V.R., Aguirre, W.E., Blacio, E., Cevallos, R., Gonzalez, M., Pozo, F., Gelwick, F., 2007. Fish communities of a disturbed mangrove wetland and an adjacent tidal river in Palmar, Ecuador. Estuar. Coast Shelf Sci. 72, 115–128.
Shimeta, J., Saint, L., Verspaandonk, E.R., Nugegoda, D., Howe, S., 2016. Long-term ecological consequences of herbicide treatment to control the invasive grass, Spartina anglica, in an Australian saltmarsh. Estuarine. Coast. Shelf Sci. 176, 58–66.
Stewart-Sinclair, P.J., Purandare, J., Bayraktarov, E., Waltham, N., Reeves, S., Statton, J., Sinclair, E.A., Brown, B.M., Shribman, Z.I., Lovelock, C.E., 2020. Blue restoration–building confidence and overcoming barriers. Front. Mar. Sci. 7, 748.
Teal, J.M., Weishar, L., 2005. Ecological engineering, adaptive management, and restoration management in Delaware Bay salt marsh restoration. Ecol. Eng. 25, 304–314.
Tuteja, N.K., Shaikh, M., 2009. Hydraulic Modelling of the Spatiio-Temporal Flood Inundation Patterns of the Koondrook Perricoota Forest Wetlands- the Living Murray, 18th World IMACS, MODSIM Congress. Modelling and Simulation Society of Australia and New Zealand, Cairns, pp. 4248–4254.
Vale, L.M., Dias, J.M., 2011. The effect of tidal regime and river flow on the hydrodynamics and salinity structure of the Lima Estuary: use of a numerical model to assist on estuary classification. J. Coast. Res. SI 64, 1604–1608.
Veitch, V., Burrows, D., Hudson, D., Butler, B., 2007. Removal of Aquatic Weeds from Lagoon Creek, Herbert Catchment North Queensland: Trialling Novel Removal Methods and Demonstration of Environmental Benefits. Australian Centre for Tropical Freshwater Research, James Cook University, Townsville, p. 51.
Wallace, J., Adame, M.F., Karim, F., Abbott, B.N., Waltham, N., 2020. Saltwater Intrustion by Removing Bund Walls to Control Invasive Aquatic Weeds on Coastal Floodplains., Report to the National Environmental Science Program Reef and Rainforest Research Centre Limited, p. 107. Cairns.
Waltham, N., Fixler, S., 2017. Aerial herbicide spray to control invasive water hyacinth (Eichhornia crassipes): water quality concerns fronting fish occupying a tropical floodplain wetland. Trop. Conserv. Sci. 10, 1940082917741592.
Waltham, N.J., Sheaves, M., 2015. Expanding coastal urban and industrial seascape in the Great Barrier Reef World Heritage Area: critical need for coordinated planning and policy. Mar. Pol. 57, 78–84.
Waltham, N.J., Burrows, D., Wegscheidl, C., Buelow, C., Ronan, M., Connolly, N., Groves, P., Audas, D., Creighton, C., Sheaves, M., 2019. Lost floodplain wetland environments and efforts to restore connectivity, habitat and water quality settings on the Great Barrier Reef. Front. Mar. Sci. 6, 71.
Waltham, N.J., Elliott, M., Lee, S.Y., Lovelock, C., Duarte, C.M., Buelow, C., Simenstad, C., Nagelkerken, I., Claassens, L., Wen, C.K., 2020. UN decade on ecosystem restoration 2021–2030—what chance for success in restoring coastal ecosystems? Front. Mar. Sci. 7, 71.
Wegscheidl, C.J., Sheaves, M., McLeod, I.M., Hedge, P.T., Gillies, C.L., Creighton, C., 2017. Sustainable management of Australia's coastal seascapes: a case for collecting and communicating quantitative evidence to inform decision-making. Wetl. Ecol. Manag. 25, 3–22.
Zahed, F., Etemad-Shahidi, A., Jabbari, E., 2008. Modeling of salinity intrusion under different hydrological conditions in the Arvand River Estuary. Can. J. Civ. Eng. 35, 1476–1480.
Zhang, X., Church, J.A., Monselesan, D., McInnes, K.L., 2017. Sea level projections for the Australian region in the 21st century. Geophys. Res. Lett. 44, 8481–8491.